



This is a repository copy of *Parametrising diffusion-taxis equations from animal movement trajectories using step selection analysis*.

White Rose Research Online URL for this paper:
<https://eprints.whiterose.ac.uk/160875/>

Version: Accepted Version

Article:

Potts, J.R. orcid.org/0000-0002-8564-2904 and Schlägel, U.E. (2020) Parametrising diffusion-taxis equations from animal movement trajectories using step selection analysis. *Methods in Ecology and Evolution*, 11 (9). pp. 1092-1105. ISSN 2041-210X

<https://doi.org/10.1111/2041-210x.13406>

This is the peer reviewed version of the following article: Potts, JR, Schlägel, UE. Parametrizing diffusion-taxis equations from animal movement trajectories using step selection analysis. *Methods Ecol Evol.* 2020; 11: 1092– 1105, which has been published in final form at <https://doi.org/10.1111/2041-210X.13406>. This article may be used for non-commercial purposes in accordance with Wiley Terms and Conditions for Use of Self-Archived Versions. This article may not be enhanced, enriched or otherwise transformed into a derivative work, without express permission from Wiley or by statutory rights under applicable legislation. Copyright notices must not be removed, obscured or modified. The article must be linked to Wiley's version of record on Wiley Online Library and any embedding, framing or otherwise making available the article or pages thereof by third parties from platforms, services and websites other than Wiley Online Library must be prohibited.

Reuse

Items deposited in White Rose Research Online are protected by copyright, with all rights reserved unless indicated otherwise. They may be downloaded and/or printed for private study, or other acts as permitted by national copyright laws. The publisher or other rights holders may allow further reproduction and re-use of the full text version. This is indicated by the licence information on the White Rose Research Online record for the item.

Takedown

If you consider content in White Rose Research Online to be in breach of UK law, please notify us by emailing eprints@whiterose.ac.uk including the URL of the record and the reason for the withdrawal request.



eprints@whiterose.ac.uk
<https://eprints.whiterose.ac.uk/>

1 Parametrising diffusion-taxis equations from animal movement
2 trajectories using step selection analysis

3 Jonathan R. Potts¹, Ulrike E. Schlägel²

4 **Short title:** Step selection for diffusion-taxis equations

5 **1** School of Mathematics and Statistics, University of Sheffield, Hicks Building, Hounsfield
6 Road, Sheffield, S3 7RH, UK; Email: j.potts@sheffield.ac.uk; Tel: +44(0)114-222-3729

7 **2** Plant Ecology and Nature Conservation, Institute of Biochemistry and Biology, University of
8 Potsdam, Am Mühlenberg 3, 14476 Potsdam, Germany; Email: ulrike.schlaegel@uni-potsdam.de

This article has been accepted for publication and undergone full peer review but has not been through the copyediting, typesetting, pagination and proofreading process, which may lead to differences between this version and the [Version of Record](#). Please cite this article as [doi: 10.1111/2041-210X.13406](https://doi.org/10.1111/2041-210X.13406)

This article is protected by copyright. All rights reserved

Abstract

1. Mathematical analysis of partial differential equations (PDEs) has led to many insights regarding the effect of organism movements on spatial population dynamics. However, their use has mainly been confined to the community of mathematical biologists, with less attention from statistical and empirical ecologists. We conjecture that this is principally due to the inherent difficulties in fitting PDEs to data.

2. To help remedy this situation, in the context of movement ecology, we show how the popular technique of step selection analysis (SSA) can be used to parametrise a class of PDEs, called *diffusion-taxis* models, from an animal's trajectory. We examine the accuracy of our technique on simulated data, then demonstrate the utility of diffusion-taxis models in two ways. First, for non-interacting animals, we derive the steady-state utilisation distribution in a closed analytic form. Second, we give a recipe for deriving spatial pattern formation properties that emerge from interacting animals: specifically, do those interactions cause heterogeneous spatial distributions to emerge and if so, do these distributions oscillate at short times or emerge without oscillations? The second question is applied to data on concurrently-tracked bank voles (*Myodes glareolus*).

3. Our results show that SSA can accurately parametrise diffusion-taxis equations from location data, providing the frequency of the data is not too low. We show that the steady-state distribution of our diffusion-taxis model, where it exists, has an identical functional form to the utilisation distribution given by resource selection analysis (RSA), thus formally linking (fine scale) SSA with (broad scale) RSA. For the bank vole data, we show how our SSA-PDE approach can give predictions regarding the spatial aggregation and segregation of different individuals, which are difficult to predict purely by examining results of SSA.

4. Our methods give a user-friendly way in to the world of PDEs, via a well-used statisti-

36 cal technique, which should lead to tighter links between the findings of mathematical ecology
37 and observations from empirical ecology. By providing a non-speculative link between observed
38 movement behaviours and space use patterns on larger spatio-temporal scales, our findings will
39 also aid integration of movement ecology into understanding spatial species distributions.

40 **Key words:** Advection-diffusion, Animal movement, Home range, Movement ecology, Partial
41 differential equations, Resource selection, Step selection, Taxis

1 Introduction

Partial differential equations (PDEs) are a principal workhorse for mathematical biologists (Murray, 2003). Their strength lies in both their utility in describing a vast range of biological systems, and the existence of many mathematical techniques for analysing them. For example, the theory of travelling wave solutions has been used to understand spreading-speeds and spatial distributions of invasive species (Kot *et al.*, 1996; Petrovskii *et al.*, 2002; Lewis *et al.*, 2016). Likewise, linear pattern formation analysis has been used for understanding animal coat patterns (Turing, 1952; Murray, 1981; Nakamasu *et al.*, 2009), vegetation stripes in semi-arid environments (Klausmeier, 1999; Sherratt, 2005), spatial predator-prey dynamics (Baurmann *et al.*, 2007; Li *et al.*, 2013), and many more examples from ecology and beyond (Kondo & Miura, 2010). There are also a variety of advanced techniques for analysing PDEs, such as asymptotic analysis, weakly non-linear analysis, energy functionals, calculus of variations, and so forth (Evans, 2010; Murray, 2012), many of which have been used in an ecological setting (Cantrell & Cosner, 2004; Eftimie *et al.*, 2009; Roques, 2013; Tulumello *et al.*, 2014; Potts & Lewis, 2016a).

Here, we are specifically interested in using PDEs to model animal movement. In this context, PDEs are valuable for understanding how patterns of utilisation distribution (the distribution of an animal's or population's space use) emerge from underlying movement processes. PDEs have been successfully applied in this regard to phenomena such as territory and home range formation (Lewis & Moorcroft, 2006; Potts & Lewis, 2014), flocking and herding (Eftimie *et al.*, 2007), organism aggregations (Topaz *et al.*, 2006), and spatial predator-prey dynamics (Lewis & Murray, 1993). They have also been used to understand animal motion in response to fluid currents (Painter & Hillen, 2015), insect dispersal (Ovaskainen *et al.*, 2008), and search strategies (Giuggioli *et al.*, 2009). In all these examples, the models are assumed to operate on timescales over which death and reproduction have minimal effect. On such timescales, the emergent spatio-temporal patterns of animal distributions are determined solely by the movement decisions of animals as they navigate the landscape. These decisions may be influenced

69 by relatively static aspects of the environment (e.g. Giuggioli *et al.* (2009); Painter & Hillen
70 (2015)) or the presence of other animals (e.g. Eftimie *et al.* (2007); Topaz *et al.* (2006)) or a
71 combination of the two (e.g. Moorcroft *et al.* (2006)).

72 Despite their broad use by applied mathematicians in general, and their great success in
73 understanding the emergent properties of ecological systems in particular, PDEs have been
74 much less-used in empirical or statistical ecology. This is perhaps due to the difficulties of
75 parametrising them from data. One can, in principle, construct a likelihood function for a PDE
76 model given the data. This has been done, for example, in mechanistic home range analysis
77 studies (Moorcroft *et al.*, 2006; Lewis & Moorcroft, 2006) and to understand insect dispersal
78 through patchy environments (Ovaskainen, 2004; Ovaskainen *et al.*, 2008). However, fitting the
79 likelihood function requires numerically solving the PDE for many different parameter values
80 (Ferguson *et al.*, 2016). Such numerics can be both time consuming and technically difficult,
81 essentially constituting a research subfield in its own right (Johnson, 2012; Ames, 2014). This
82 is especially true when there are multiple interacting populations, due to the inherent non-
83 linearities in the resulting PDEs, and also when the datasets are very large, as is increasingly
84 the case (Hays *et al.*, 2016).

85 To test the theoretical advancements of PDE research against empirical observations, it is
86 thus necessary to develop quicker and technically simpler methods for parametrisation. Sev-
87 eral such methods have been developed to this end. For example, homogenisation techniques
88 have been recently developed to simplify numerical solutions of reaction-diffusion equations (a
89 class of PDEs), by separating time-scales in a biologically-motivated way (Powell & Zimmer-
90 mann, 2004; Garlick *et al.*, 2011). Hefley *et al.* (2017) combined these methods with Bayesian
91 techniques to parametrise reaction-diffusion equations efficiently and accurately from data on
92 animal locations and disease transmission. However, these techniques rely on there being a
93 biologically meaningful way to separate spatio-temporal scales, which is system-dependent.
94 Furthermore it still requires numerical solutions of PDEs (albeit simplified ones), with all the
95 technical baggage they can engender.

96 Likewise, the technique of gradient matching can also be used for rapid inference of differ-
97 ential equation models (Xun *et al.*, 2013; Macdonald & Husmeier, 2015). However, whilst this
98 method can speed-up inference considerably, applying it to a movement trajectory (as is our
99 present concern) requires interpolating between the data-points to give a smooth utilisation
100 distribution. Indeed, the accuracy of the inference can be highly dependent upon the choice of
101 this smoothing (Ferguson, 2018). Therefore it is necessary, when applying gradient matching
102 to a trajectory, to try various smoothing procedures, which can be time consuming. Then,
103 only if the procedures give similar results can one be confident about the outcome. As a con-
104 sequence, gradient matching is best suited to data where there are sufficiently many individual
105 organisms that the utilisation distribution can be reliably estimated with high accuracy, e.g.
106 when studying cell aggregations (Ferguson *et al.*, 2016). However, in many studies of vertebrate
107 animals' movements, only a limited number of individuals can be tracked. It would therefore
108 be advantageous to find a simpler, robust method of inference for parametrising PDEs, tailored
109 to such animal tracking data.

110 To fill this gap, we show here that the oft-used technique of step selection analysis (Fortin
111 *et al.*, 2005; Forester *et al.*, 2009; Thurfjell *et al.*, 2014; Avgar *et al.*, 2016) can be used to
112 parametrise a class of PDEs called *diffusion-taxis equations* from animal tracking data. These
113 are examples of advection-diffusion equations (sometimes called convection-diffusion) where the
114 advection is up or down a gradient of some physical quantity (e.g. a gradient of resources). Such
115 PDEs can describe animal movement in relation to external factors (e.g. landscape features or
116 con- or hetero-specific individuals) and hence make them a suitable model for animal movement
117 in many situations. Step selection analysis (SSA) is already very widely-used, being both fast
118 and simple to implement. Indeed, implementation has recently become even simpler thanks to
119 the release of the `amt` package in R (Signer *et al.*, 2019), so using our method does not require
120 significant new technical understanding by practitioners.

121 The diffusion-taxis equations we consider consist of two terms: (i) the diffusion term, which
122 denotes the tendency for the animal locations to spread through time, and (ii) the taxis term,

123 which encodes drift tendencies in the animal's movement. Both terms may, in principle, vary
124 across space, in particular in response to external factors such as habitat features, resources,
125 predators, or conspecific individuals. As such, this is a very intuitive way to think about animal
126 movement (Ovaskainen, 2004).

127 In this work, we give a simple recipe for converting the output of SSA into parameters for
128 a diffusion-taxis equation. We then show how to use systems of such equations to understand
129 both quantitative and qualitative features of emergent space-use patterns. In particular, we
130 demonstrate how to derive the steady-state utilisation distribution (UD) in certain cases. This
131 UD can be written in a closed-form, analytic expression, obviating the need for time-consuming
132 numerics (Signer *et al.*, 2017). It describes the long-term space use of animals (i.e. their home
133 ranges) and, in contrast to the mere SSA-derived parameter values, can be used to make
134 rigorous predictions about space-use (Moorcroft & Barnett, 2008; Potts & Lewis, 2014). We
135 also show how to predict whether the UD of an individual animal or a population is likely to
136 either (i) tend to a uniform steady-state (animal spread homogeneously across the landscape),
137 (ii) reach a steady state with aggregation or segregation patterns, or (iii) be in perpetual
138 spatio-temporal flux, never reaching a steady state.

139 Knowing when these emergent spatial distributions may arise from movement processes is
140 vital for understanding spatial distributions of individuals within a population and ultimately
141 species distributions. Individuals often use non-diffusive movement mechanisms (e.g. spatially
142 explicit selection of locations based on resources or presence of conspecifics) which scale up
143 to different space-use patterns such as homogeneous mixing, spatial aggregation/segregation,
144 or dynamic spatio-temporal patterns (Potts & Lewis, 2019). Such movement decisions and
145 resulting patterns challenge the assumption of well-mixed populations in traditional population
146 models. This also has implications for demography, for example via density dependence or
147 carrying capacities (Morales *et al.*, 2010; Riotte-Lambert *et al.*, 2017; Spiegel *et al.*, 2017), as
148 well as interspecific interactions in communities such as competition (Macandza *et al.*, 2012;
149 Vanak *et al.*, 2013). As such, we encourage increased research effort in examining the effects of

150 movement mechanisms on spatial patterns. We propose the tools developed through this paper
 151 and Schlägel *et al.* (2019) as a means to aid such examination. Although the mathematical
 152 justification for the techniques given here requires some technical expertise, the recipes for
 153 implementing these techniques do not require advanced mathematical understanding (being
 154 SSA plus some minimal post-processing), so have potential to be widely applied.

155 2 Methods

156 2.1 From step selection to diffusion-taxis

157 Suppose an animal is known to be at location \mathbf{x} at time t . Step selection analysis (SSA)
 158 parametrises a probability density function, $p_\tau(\mathbf{z}|\mathbf{x}, t)$, of the animal being at location \mathbf{z} at
 159 time $t + \tau$, where τ is a time-step that usually corresponds to the time between successive
 160 measurements of the animal's location (Forester *et al.*, 2009). For our purposes, the functional
 161 form of $p_\tau(\mathbf{z}|\mathbf{x}, t)$ is as follows

$$162 \quad p_\tau(\mathbf{z}|\mathbf{x}, t) = K^{-1}(\mathbf{x}, t)\phi_\tau(|\mathbf{z} - \mathbf{x}|) \exp[\beta_1 Z_1(\mathbf{z}, t) + \dots + \beta_n Z_n(\mathbf{z}, t)]. \quad (1)$$

164 Here, $\phi_\tau(|\mathbf{z} - \mathbf{x}|)$ is the step length distribution (i.e. a hypothesised distribution of distances
 165 that the animal travels in a time-step of length τ), $|\mathbf{z} - \mathbf{x}|$ is the Euclidean distance between
 166 \mathbf{z} and \mathbf{x} , $\mathbf{Z}(\mathbf{z}, t) = (Z_1(\mathbf{z}, t), \dots, Z_n(\mathbf{z}, t))$ is a vector of spatial features that are hypothesised
 167 to co-vary with the animal's choice of next location, $\boldsymbol{\beta} = (\beta_1, \dots, \beta_n)$ is a vector denoting the
 168 strength of the effect of each $Z_i(\mathbf{z}, t)$ on movement, and

$$169 \quad K(\mathbf{x}, t) = \int_{\Omega} \phi_\tau(|\mathbf{z} - \mathbf{x}|) \exp[\beta_1 Z_1(\mathbf{z}, t) + \dots + \beta_n Z_n(\mathbf{z}, t)] d\mathbf{z} \quad (2)$$

171 is a normalising function, ensuring $p_\tau(\mathbf{z}|\mathbf{x}, t)$ integrates to 1 (so is a genuine probability density
 172 function). In Equation (2), Ω is the study area, which we assume to be arbitrarily large.
 173 We also require that the step-length distribution, $\phi_\tau(|\mathbf{z} - \mathbf{x}|)$, not be heavy-tailed (i.e. its

174 mean, variance, and all its other moments must be finite). The parameters β_1, \dots, β_n are then
175 the focus of an SSA, indicating the selection behaviour of animals towards spatial features
176 of their environment. We refer to the function $\exp[\beta_1 Z_1(\mathbf{z}, t) + \dots + \beta_n Z_n(\mathbf{z}, t)]$ as a step
177 selection function (SSF), in line with its first use in the literature (Fortin *et al.*, 2005). Note,
178 though, that sometimes the term SSF is instead used for the entire probability density function
179 (Equation 1) (Forester *et al.*, 2009). In either case, SSA is the method of parametrising an
180 SSF to analyse animal movement data. Note also that the functional form of Equation (1) is
181 analogous to the weighted distribution approach to resource selection analysis (Johnson *et al.*,
182 2008b; Wijeyakulasuriya *et al.*, 2019).

183 One can generalise Equations (1-2) by incorporating environmental effects across the whole
184 step from \mathbf{x} to \mathbf{z} , not just the end of the step at \mathbf{z} . Furthermore, one can model autocorrelation
185 in movement via turning angle distributions (Forester *et al.*, 2009; Avgar *et al.*, 2016). For
186 the sole purpose of parametrising an advection-diffusion PDE, though, it is not necessary to
187 model either of these considerations, so we use the functional form in Equation (1). However,
188 it is worth being aware that, should data be highly autocorrelated (e.g. if the turning angle
189 distribution is far from uniform), the resulting inference may be inaccurate. We return to the
190 issue of autocorrelation in more detail in the Discussion, and discuss how to ensure a given
191 dataset is suitable for the methods presented here.

192 The SSA method requires data on a sequence of animal locations $\mathbf{x}_1, \dots, \mathbf{x}_N$ gathered at
193 times t_1, \dots, t_N respectively (with $t_{j+1} - t_j = \tau$ for all j , so that the time-step is constant),
194 together with a vector of environmental layers, $\mathbf{Z}(\mathbf{z}, t_j)$ at each time-point t_j . It then returns
195 best-fit values for the parameters β_1, \dots, β_n , using a conditional logistic regression technique,
196 by comparing each location with a set of ‘control’ locations sampled from an appropriate
197 probability distribution, which represents locations that would be available to the animal based
198 on its movement capabilities. Details of the SSA technique and how it should be implemented
199 are given in previous works, e.g. Thurfjell *et al.* (2014); Avgar *et al.* (2016), so we omit them
200 here. Note that alternative approaches to parameter estimation for Equation (1) are also

possible, for example using maximum likelihood estimation or Bayesian techniques (Johnson *et al.*, 2008b; Wijeyakulasuriya *et al.*, 2019).

We wish to use the SSA output to parametrise a diffusion-taxis model of the probability density function of animal locations, given by $u(\mathbf{x}, t)$. Notice that $u(\mathbf{x}, t)$ is different to the distribution described by Equation (1), which gives the probability density function of moving to location \mathbf{z} , conditional on currently being located at \mathbf{x} . However, in Supplementary Appendix A, we show that under the model in Equation (1), and as long as τ is sufficiently small, $u(\mathbf{x}, t)$ is well-described by the following diffusion-taxis equation

$$\frac{\partial u}{\partial t} = \underbrace{D_\tau \nabla^2 u}_{\substack{\text{diffusive} \\ \text{movement}}} - \underbrace{2D_\tau \nabla \cdot [u \nabla (\beta_1 Z_1 + \dots + \beta_n Z_n)]}_{\substack{\text{drift up the gradient} \\ \text{of } \beta_1 Z_1 + \dots + \beta_n Z_n}}. \quad (3)$$

Here, $\nabla = (\partial/\partial x, \partial/\partial y)$ (where $\mathbf{x} = (x, y)$), and

$$D_\tau = \frac{1}{4\tau} \int_{\mathbb{R}^2} |\mathbf{x}|^2 \phi_\tau(|\mathbf{x}|) d\mathbf{x}, \quad (4)$$

is a constant that describes the rate of diffusive movement. The derivation makes use of a diffusion-approximation approach (Turchin, 1998), whereby $u(\mathbf{x}, t)$ is derived by a moment-closure technique from a recurrence equation that describes how an animal's location arises from its previous locations, and $p(\mathbf{z}|\mathbf{x})$ specifies the probability density of a specific movement step.

The drift part of Equation (3) describes animal movement in a preferred direction according to environmental features, whereas the diffusive part takes care of small-scale stochasticity due to any other factors not accounted for explicitly. For this approximation to work, the time step τ must be sufficiently small that the gradient of resources (in any fixed direction) does not vary greatly across the spatial extent over which an animal is likely to move in time τ (see Supplementary Appendix A for precise mathematical details, and the Discussion for more on

dealing with situations where this assumption is violated).

For our analysis, it is convenient to work in dimensionless co-ordinates. To this end, we start by setting $\tilde{\mathbf{x}} = \mathbf{x}/x_*$ to be dimensionless space, where x_* is a characteristic spatial scale. Since, in practice, the functions $Z_i(\mathbf{x}, t)$ arrive as rasterised layers (i.e. square lattices), it is convenient to let x_* be the pixel width (or, synonymously, the lattice spacing), but in principle the user can choose x_* arbitrarily. We also set $\tilde{t} = tD_\tau/(x_*)^2$ and $\tilde{u} = (x_*)^2u$. Then, immediately dropping the tildes above the letters for notational convenience, Equation (3) has the following dimensionless form

$$\frac{\partial u}{\partial t} = \nabla^2 u - 2\nabla \cdot [u\nabla(\beta_1 Z_1 + \dots + \beta_n Z_n)]. \quad (5)$$

In summary, we have shown that step selection analysis can be used to parametrise a diffusion-taxis equation (Equation 5) where the drift term consists of taxis up the gradient of any covariate Z_i for which β_i is positive, and down the gradient of any covariate Z_j for which β_j is negative.

The key value in moving from the movement kernel in Equation (1) to the PDE in Equation (5) is that it allows us to make an explicit connection between a model, $p_\tau(\mathbf{z}|\mathbf{x}, t)$, of movement decisions over a small time interval, τ , and the predicted probability distribution, $u(\mathbf{x}, t)$, of an animal's location at any point in time. While SSA by itself only gives inference about the movement rules themselves, the resulting PDEs enable us to make predictions of the space use patterns that will emerge over time, should the animal be moving according to the rules of the parametrised movement kernel (cf. Signer *et al.* (2017); Wilson *et al.* (2018)). Examples of such patterns, including steady-state home ranges, aggregation, and segregation, will be demonstrated later in this manuscript.

2.2 Assessing inference accuracy on simulated data

To test the reliability of our parametrisation technique, we simulate paths given by diffusion-taxis equations of the general form in Equation (5). We then use step selection analysis to see

251 whether the inferred β parameters match those that we used for simulations. For this study,
 252 we simulate two different types of model. In the first, which we call the *Fixed Resource Model*,
 253 there is just one landscape layer (so $n = 1$) and $Z_1(\mathbf{x}, t) = Z_1^f(\mathbf{x})$ is a raster of resource values
 254 that does not vary over time (the superscript f emphasises that we are using the Fixed Resource
 255 Model). This raster is a Gaussian random field, constructed using the `RMGauss` function in the
 256 `RandomFields` package for R, with the parameter `scale=10` (Fig. 1a).

257 The second model is called the *Home Range Model*. This has $n = 2$ (i.e. two landscape
 258 layers), the first of which, $Z_1^h(\mathbf{x}) = Z_1^f(\mathbf{x})$, is the random field from Fig. 1a (the superscript h
 259 emphasises that we are working with the Home Range Model). The second denotes a tendency
 260 to move towards the central point on the landscape, which may be a den or nest site for the
 261 animal. This has the functional form $Z_2^h(\mathbf{x}) = -|\mathbf{x}_c - \mathbf{x}|$, where \mathbf{x}_c is the centre of the landscape.
 262 Notice that ∇Z_2^h is an identical advection term to that in the classical Holgate-Okubo localising
 263 tendency model (Holgate, 1971; Lewis & Moorcroft, 2006).

264 For each of these two models, we simulate trajectories from Equation (5) for a variety of
 265 β -values. Each trajectory consists of 1,000 locations, gathered at dimensionless time-intervals
 266 of $\tau = 1$. (Recall from the non-dimensionalisation procedure that this corresponds to a time
 267 of x_*^2/D where x_* is the pixel width and D the diffusion constant of the animal, defined
 268 in Equation 4). We construct 10 trajectories for each β -value used. Details of the method
 269 used for generating trajectories are given in Supplementary Appendix B. In short, the method
 270 involves reverse-engineering a stochastic individual-based model (IBM) from the PDE, such
 271 that the probability distribution of stochastic realisations of the IBM evolves in accordance
 272 with Equation (5). For the Fixed Resource Model, we also perform the same procedure but
 273 fixing $\beta_1^f = 1$ and varying τ , to understand the effect on inference of the time step, τ , at which
 274 data are gathered.

275 We then parametrise each trajectory using SSA, finding control locations by sampling steps
 276 from a bivariate normal distribution with zero mean and a standard deviation equal to the
 277 empirical standard deviation. We match each case to 100 controls. To determine whether SSA

is effective in parametrising diffusion-taxis equations, we test whether the inferred β -values fall within 95% confidence intervals of the values used to simulate the trajectories.

2.3 Application to empirical data and spatial pattern formation

To demonstrate the utility of diffusion-taxis models for animal movement, we used some recent results from a study of social interactions between bank voles (*Myodes glareolus*), reported by Schlägel *et al.* (2019). This study used SSA to infer the movement responses of each individual in a group to the other individuals. For example, individual 1 may tend to be attracted towards 2, who in turn may like to avoid 1 but rather be attracted towards 3. In the studied bank voles, such individualistic responses arose as sex-specific behaviours likely related to mating. However, they may also arise in relation to social foraging or interactions between species in competitive guilds.

Details of the method are given in Schlägel *et al.* (2019), but here we give the ideas pertinent to the present study. Suppose there are M individuals in a group. For each individual, $i \in \{1, \dots, M\}$, consider the utilisation distribution of each of the other individuals to be a landscape layer. In other words $Z_j(\mathbf{x}, t) = u_j(\mathbf{x}, t)$ in the step selection function (Equation 1). It may not be immediately obvious that one individual may be able to have knowledge about another's utilisation distribution, but there are at least two biological processes by which this can happen, both of which can be justified mathematically (Potts & Lewis, 2019). The first is for individuals to mark the terrain as they move (e.g. using urine or faeces) and then the distribution of marks mirrors the utilisation distribution (Gosling & Roberts, 2001; Potts & Lewis, 2016b). The second is for animals to remember past interactions with other individuals and respond to the cognitive map of these interactions (Fagan *et al.*, 2013; Potts & Lewis, 2016a).

By Equation (5), these movement processes give rise to a system of diffusion-taxis equations, one for each individual in the group, that each have the following form (in dimensionless co-

303 ordinates)

$$304 \quad \frac{\partial u_i}{\partial t} = \nabla^2 u_i - 2\nabla \cdot \left[u_i \nabla \sum_{j \neq i} \beta_{i,j}^v u_j \right]. \quad (6)$$

306 Here, $\beta_{i,j}^v$ measures the tendency for individual i to move either towards (if $\beta_{i,j}^v > 0$) or away
 307 from (if $\beta_{i,j}^v < 0$) individual j . The magnitude of $\beta_{i,j}^v$ measures the strength of this advective
 308 tendency. These correspond to the β -values inferred by SSA, with a superscript v to emphasise
 309 that these refer to the bank vole study.

310 Depending on the values of $\beta_{i,j}^v$, such a system of diffusion-taxis equations can have rather
 311 rich dynamics. These dynamics can be observed through numerical simulations (Fig. 2b).
 312 However, for technical reasons, to perform numerics we have to replace u_j in Equation (6)
 313 with a locally-averaged version $\bar{u}_j = \int_{B(\mathbf{x})} u_j(\mathbf{z}) d\mathbf{z}$, where $B(\mathbf{x})$ is a small neighbourhood of \mathbf{x} .
 314 This is to avoid rapid growth of small perturbations at arbitrarily high frequencies, which can
 315 happen without spatial averaging [see Supplementary Appendix D and Potts & Lewis (2019)
 316 for details]. The system we simulate is thus as follows

$$317 \quad \frac{\partial u_i}{\partial t} = \nabla^2 u_i - 2\nabla \cdot \left[u_i \nabla \sum_{j \neq i} \beta_{i,j}^v \bar{u}_j \right]. \quad (7)$$

319 Details of the numerics are given in Supplementary Appendix D. To demonstrate some of
 320 the patterns that can emerge, Fig. 2 displays the spatio-temporal dynamics of the system in
 321 Equation (7) for various example parameter values. In Fig. 2a,b, we have $M = 3$, $\beta_{1,2}^v = -2$,
 322 $\beta_{1,3}^v = -0.5$, $\beta_{2,1}^v = 0.5$, $\beta_{2,3}^v = 2$, $\beta_{3,1}^v = 0.5$, $\beta_{3,2}^v = 0.5$. This means that Individual 1 is
 323 avoiding both 2 ($\beta_{1,2}^v = -2$) and 3 ($\beta_{1,3}^v = -0.5$); however 2 and 3 are both attracted towards 1
 324 ($\beta_{2,1}^v = 0.5$, $\beta_{3,1}^v = 0.5$) and also each other ($\beta_{2,3}^v = 2$, $\beta_{3,2}^v = 0.5$). This complicated three-way
 325 relationship turns out to cause perpetually oscillating spatial patterns (Fig. 2a,b).

326 In Fig. 2c,d, we have $M = 3$, $\beta_{1,2}^v = -2$, $\beta_{1,3}^v = -0.5$, $\beta_{2,1}^v = 0.5$, $\beta_{2,3}^v = -2$, $\beta_{3,1}^v =$
 327 0.5 , $\beta_{3,2}^v = 0.5$. Thus Individual 1 still avoiding both 2 ($\beta_{1,2}^v = -2$) and 3 ($\beta_{1,3}^v = -0.5$).

328 Furthermore, 2 and 3 are both still attracted towards 1 ($\beta_{2,1}^v = 0.5$, $\beta_{3,1}^v = 0.5$) and 3 is
 329 attracted to 2 ($\beta_{3,2}^v = 0.5$). However, this time 2 is avoiding 3 ($\beta_{2,3}^v = 2$). This situation leads
 330 to stationary spatial patterns (Fig. 2c,d).

331 It is perhaps not immediately obvious why this simple switch in behaviour from 2 being
 332 attracted to 3 to 2 avoiding 3 should have such a dramatic change in the qualitative nature
 333 of the utilisation distributions. However, one can gain insight into such effects by using linear
 334 pattern formation analysis (Turing, 1952). This technique separates parameter space into three
 335 regions: (a) *No Patterns*, so each individual will eventually use all parts of space with equal
 336 probability, (b) *Stationary Patterns*, where individual utilisation distributions form spatially-
 337 heterogeneous patterns that typically lead to spatial segregations (with some possible overlap)
 338 and/or aggregations in certain parts of space (Fig. 2c-d), (c) *Oscillatory Patterns*, where small
 339 spatially-heterogenous perturbations oscillate and grow, meaning spatial patterns remain in
 340 perpetual flux (Fig. 2a-b).

341 These parameter regimes are easily determined by calculating the eigenvalues of a matrix
 342 A , calculated in Potts & Lewis (2019) for Equation (7), which we call the *pattern formation*
 343 *matrix*. This matrix has diagonal entries $A_{ii} = -1$ (for $i = 1, \dots, M$) and the entry in the
 344 i -th row and j -th column is $A_{ji} = -2\beta_{i,j}^v$ for $i \neq j$. If the real parts of the eigenvalues of A
 345 are all negative then we are in the *No Pattern* parameter regime. If there is an eigenvalue
 346 whose real part is positive and the eigenvalue with the largest real part (a.k.a. the *dominant*
 347 *eigenvalue*) is a real number, then this is the *Stationary Patterns* regime. Otherwise, we are in
 348 the *Oscillatory Patterns* regime, where the dominant eigenvalue is non-real. These eigenvalues
 349 can be calculated in most computer packages, so there is no need for specialist mathematical
 350 knowledge. For example, the R programming language has a function `eigen()` designed for this
 351 purpose. Step-by-step instructions for the whole procedure of determining pattern formation
 352 properties are given in Supplementary Appendix C.

353 In Schlägel *et al.* (2019), $\beta_{i,j}^v$ -values were inferred using SSA in all cases where i and j were
 354 of different sex, for eight different replicates (see Fig. 4 in their paper). Here, we use the

published best-fit values to construct the pattern formation matrix, A , for each of the eight replicates. We use this to categorise each replicate by its pattern formation properties (No Patterns, Stationary Patterns, Oscillatory Patterns).

3 Results

3.1 Simulated data

When tested against simulated trajectories from diffusion-taxis equations, SSA was generally reliable at returning the parameter values used in the simulations (Fig. 1). For the Fixed Resource Model, there was just one parameter, $\beta_1 = \beta_1^f$ (the superscript denoting the Fixed Resource Model). All but one of the real values lay within the corresponding 95% confidence intervals of the SSA-inferred values (Fig. 1b). The one that did not ($\beta_1^f = 5$) was only slightly out, so this may have been simply due to random fluctuations. SSA tended to slightly overestimate the value of β_1^f with this resource layer, particularly for higher β_1^f values. However, since the difference between the inferred value of β_1^f and the actual value is never very large, and within the margin of error for each individual value of β_1^f , this suggests the approximations inherent in the derivation of Equation (5) from Equation (1) are acceptable for practical purposes. Fig. 1c shows the practical outcome of the small- τ requirement, whereby the inference over-estimates β_1^f as τ increases. Notice also that, if τ is too small, the inference has large error bars, owing to minimal change in resources over the spatial extent the animal travels in time τ , making it hard for the SSA procedure to return a precise signal.

The SSA inference performed on the Home Range Model returned β -values whose 95% confidence intervals contained the real values in $> 90\%$ of cases. Those cases where the real values lay outside the confidence intervals were always only marginally outside (Fig. 1e,f; Supplementary Fig. SF1). However, as with the Fixed Resource Model, there is a tendency for SSA to slightly overestimate the real values of $\beta_1 = \beta_1^h$ (superscript h for Home Range Model). The estimation of β_2^h tends to be quite close to the real value unless β_1^h is rather large, at which

380 point SSA starts to over-estimate β_2^h very slightly yet consistently (Supplementary Fig. SF1).

381 For the Home Range Model, it is interesting to examine the long-term utilisation distribu-
 382 tion of the animal's probability distribution, i.e. its home range. A steady-state distribution
 383 for Equation (5) is given by

$$384 \quad u_*(\mathbf{x}) = C^{-1} \exp[2\beta_1 Z_1(\mathbf{x}) + \dots + 2\beta_n Z_n(\mathbf{x})], \quad (8)$$

386 where $C = \int_{\Omega} \exp[2\beta_1 Z_1(\mathbf{x}, t) + \dots + 2\beta_n Z_n(\mathbf{x}, t)] d\Omega$ is a normalising constant ensuring $u_*(\mathbf{x})$
 387 integrates to 1, so is a probability density function. That Equation (8) is a steady-state of
 388 Equation (5) can be shown by placing $u(\mathbf{x}, t) = u_*(\mathbf{x})$ into the right-hand side of Equation (5)
 389 and showing it vanishes. Note the factor of 2 before all the β_i in Equation (8), a phenomenon
 390 that occurred for the same reasons in a 1D version of Equation (8) in Moorcroft & Barnett
 391 (2008), where they comment on the mathematical and biological reasons behind this. Fig. 1d
 392 gives the result of plotting Equation (8) for the Home Range model with parameter values
 393 $\beta_1 = \beta_1^h = 1$, $\beta_2 = \beta_2^h = 0.1$. This shows how empirically-parametrised diffusion-taxis models
 394 can be used to predict home range size and shape.

395 3.2 Bank vole data

396 Table 1 shows the best-fit $\beta_{i,j}^v$ -values inferred by Schlägel *et al.* (2019), together with the
 397 resulting dominant eigenvalues of the pattern formation matrix. Of the eight replicates, two of
 398 them were in the region where no patterns form, six where there are stationary patterns, but
 399 none where we predict oscillatory patterns.

400 Here, Individuals 1 and 2 are female, whilst 3 and 4 are male. A positive number for $\beta_{i,j}^v$
 401 means that Individual i tends to move towards j (more precisely, i moves up the gradient of
 402 the utilisation distribution of j). For example, in Replicate A, the sole female has a tendency
 403 to move towards both males and this attraction is reciprocated. Our mathematical analysis
 404 suggests that the steady-state utilisation distribution will likely be non-uniform. One would
 405 expect, given the mutual attraction, that this would result in an aggregation of all three

Table 1. Pattern formation in bank vole populations. The first column labels the eight replicates A-H, following Schlägel *et al.* (2019). The next eight columns give the $\beta_{i,j}^v$ -values (as defined for Equation 6) which are the best-fit values from Schlägel *et al.* (2019, Fig. 4). The penultimate column gives the dominant eigenvalue of the linearised system and the final column gives the patterning regime predicted by linear pattern formation analysis of the system of Equations (6).

Replicate	$\beta_{1,3}^v$	$\beta_{1,4}^v$	$\beta_{2,3}^v$	$\beta_{2,4}^v$	$\beta_{3,1}^v$	$\beta_{3,2}^v$	$\beta_{4,1}^v$	$\beta_{4,2}^v$	Eigenvalue	Pattern regime
A	0.3	0.5	N/A	N/A	0.5	N/A	0.5	N/A	0.26	Stationary
B	0.4	-1	0.8	-0.1	0.5	0.8	0.3	-0.4	0.94	Stationary
C	-0.6	0.9	N/A	N/A	0.3	N/A	0.2	N/A	-1.0	None
D	-2.9	-5.2	N/A	N/A	0.6	N/A	0.9	N/A	-1.0+5.1i	None
E	0.7	0.7	-1.4	0.7	0.6	-0.5	0.4	0.2	1.1	Stationary
F	0.8	1.3	0.1	-0.1	0.7	-0.4	1.2	-0.1	1.9	Stationary
G	-1.2	0.4	1.4	1.3	-0.4	1	0.8	1.3	2.4	Stationary
H	0.6	0.1	N/A	N/A	0.8	N/A	0.4	N/A	0.44	Stationary

406 individuals in Replicate A. In Figs. 3a,b, we confirm this by numerically solving the diffusion-
 407 taxis equations from Equation (7) with the parameter values from the first row of Table 1 in
 408 a simple 1D domain. Note that the width of the aggregations is dependent upon the size of
 409 the spatial averaging kernel, $B(x)$, and the exact positions of the aggregations are dependent
 410 on initial conditions (Potts & Lewis, 2019, Fig. 5). Despite this existence of multiple steady-
 411 state solutions, the general aggregation or segregation properties of the system appear to be
 412 independent of initial condition. This is proved for a simple $N = 2$ case in Potts & Lewis
 413 (2019, Sec. 4.1) and numerical evidence given for situations away from that case.

414 In Replicates B, E, and F, stationary patterns are predicted to form, but the attract-
 415 and-avoid dynamics are rather more complicated, making prediction of the aggregation or
 416 segregation properties difficult to predict simply by eye-balling the $\beta_{i,j}^v$ -values. Numerical
 417 analysis shows that Individuals 1, 2, and 3 (both females and one male) in Replicate B tend to
 418 occupy approximately the same part of space, but that Individual 4 (the other male) tends to
 419 use the other parts of space (Fig. 3c,d).

420 In Replicate E, the attract/avoid dynamics given in Schlägel *et al.* (2019) show three mutu-
 421 ally attractive pairings: (1,3), (1,4), (2,4) (Table 1). This, by itself, would suggest aggregation

422 of all four individuals. However, we also see that Individuals 2 and 3 are mutually *avoiding*,
423 so it is not immediately obvious what the space use patterns should look like. We therefore
424 require a numerical solution of the diffusion-taxis equations, as given in Fig. 3e,f. This reveals
425 a three-way aggregation of both males (Individuals 3 and 4) and one female (Individual 1).
426 The remaining female (Individual 2) strongly avoids the other three individuals, sticking to
427 parts of space that are hardly ever used by 1, 3, and 4.

428 Replicate F likewise reveals complicated relationships between the four individuals. Here,
429 numerical analysis of the corresponding diffusion-taxis system reveals an aggregation of both
430 males (Individuals 3 and 4) and one female (Individual 1), similar to Replicate E. This time,
431 however, Individual 2 (female) uses all parts of space, with very little tendency to avoid the
432 others.

433 Replicates G and H are similar in nature to E and A, respectively. Like E, Replicate G has
434 three mutually-attractive pairings, (1,4), (2,3), and (3,4), and one mutually avoiding pairing,
435 (1,3). The corresponding spatial patterns (not shown) reveal aggregation of Individuals 2, 3,
436 and 4, with Individual 1 using other parts of space. Replicate H has mutual attraction between
437 all three individuals and, as such, leads to space use patterns (not shown) of mutual aggregation
438 between the three individuals.

439 Finally, it is worth stressing that the diagrams in Fig. 3 are only there to demonstrate
440 qualitative features of space use that diffusion-taxis analysis predicts will emerge. Principally,
441 these are to understand whether the spatial patterns that emerge are of segregation or aggre-
442 gation. However, these diagrams are not meant to represent accurate predictions of spatial
443 patterns. Accurate predictions of space use would require incorporating into the model all the
444 relevant resource distributions and environmental features (e.g. those in Section 2.2), together
445 with empirically realistic initial conditions and spatial averaging kernel, in addition to details
446 of between-individual interactions.

4 Discussion

We have demonstrated how diffusion-taxis equations can be parametrised from animal movement data, using the well-used and user-friendly technique of step selection analysis. The utility of such models is evidenced through two examples: (I) constructing the steady-state utilisation distribution (UD), thus relating the underlying movement to the long-term spatial distribution of a population, and (II) examining whether spatial patterns in the utilisation distribution will form spontaneously and whether these will be stable or in perpetual flux.

Despite relying on the mathematical theory of PDEs, both examples can be used without any specialist mathematical knowledge. The formula for the UD is given in a simple closed form (Equation 8), so practitioners simply need to perform SSA on their path, then plug the resulting β_i -values into Equation (8) to infer the UD. This builds on a 1-dimensional result from Moorcroft & Barnett (2008) by generalising it to higher dimensions and linking it explicitly to the functional form given by the output of SSA. The classification of spatial distributions into ‘No Patterns’, ‘Stationary Patterns’, and ‘Oscillatory Patterns’ is done by (a) placing the $\beta_{i,j}$ -values into the matrix A , described in Section 2.3, then (b) calculating the eigenvalues, for example using the `eigen()` package in R. This can all be done without the need to perform technical mathematical calculations.

Our results linking the output of step selection analysis to the steady state utilisation distribution (Equation 8) are of direct application to mechanistic home range analysis (Lewis & Moorcroft, 2006). Traditionally, these were fitted to data by numerically solving a system of PDEs for a range of parameter values and searching for the best fit: a time-consuming process that requires technical knowledge of numerical PDEs. Our method, in contrast, simply requires the requisite knowledge to perform conditional logistic regression, which is both relatively quick and well-known.

The result of Equation (8) also makes a simple, formal link between the step selection function (SSF) and the UD that emerges from the SSF, which has an exponential form, similar to a resource selection function (RSF). This question of the UDs emerging from an SSF was

474 examined using individual-based simulations by Signer *et al.* (2017), but our work makes this
475 connection analytic in the case where the selection only depends on the end of the step and the
476 turning angle distribution is uniform. Previous attempts to make this connection have started
477 with an exponential form for the SSF and derived a rather more complicated equation for the
478 UD (Barnett & Moorcroft, 2008; Potts *et al.*, 2014). A more recent attempt works the other
479 way around: beginning with an exponential formulation for the UD, then deriving a movement
480 kernel that gives the UD in the appropriate long-term limit (Michelot *et al.*, 2018). However,
481 the resulting movement kernel does not appear in an exponential form like Equation (1). Our
482 approach, although it relies on limiting approximation, has both a movement kernel (Equation
483 1) and a utilisation distribution in a similar, exponential form (Equation 8). In some sense,
484 this is just a trivial extension of the 1D result of Moorcroft & Barnett (2008), but a useful one
485 that has not been made explicit in the literature.

486 Since the predicted UD from Equation (8) is in an exponential form, similar to an RSF,
487 it is quite straightforward for practitioners to estimate the error in this prediction and gain
488 useful biological information about drivers of space-use patterns. First, one would subsample
489 the data to give relocations that can be reasonably considered as independent. Then, one can
490 re-parametrise Equation (8) using resource selection analysis on these relocation data. The
491 β_i -values from this re-parametrisation can then be compared with those from the SSA-PDE
492 procedure described here.

493 Our results related to spontaneous pattern formation (Example II) are of particular im-
494 portance with regards to species distribution modelling. These results build upon the studies
495 of Potts & Lewis (2019) and Schlägel *et al.* (2019). The former study demonstrates the wide
496 variety of population distribution patterns that can emerge from taxis up or down utilisa-
497 tion distribution gradients of other animals (including aggregation, segregation, oscillatory,
498 and irregular patterns), whilst the latter gives a method for parametrising SSFs that describe
499 movement responses to such gradients. The key novelty of our work with respect to the previ-
500 ous two is to demonstrate how the output of SSA, including from the specific SSA techniques of

501 Schlägel *et al.* (2019), can be used to parametrise diffusion-taxis equations of the type studied
502 in Potts & Lewis (2019). With this, we here provide the means to bridge the gap between in-
503 ference on the mechanisms of fine-scale movement decisions (SSA) and predictions on resulting
504 space-use patterns (PDEs).

505 Despite the wealth of theoretical work on pattern formation in animal populations over
506 many decades [e.g. Levin (1974); Chesson (1985); Durrett & Levin (1994); Baurmann *et al.*
507 (2007); Li *et al.* (2013)], spontaneous pattern formation is an aspect of animal space use typi-
508 cally ignored in species distribution models, which principally concern themselves with relating
509 space use to environmental features. However, the literature on pattern formation gives many
510 examples of features of spatial distributions that can arise without any need for correlation
511 with environmental features. Perhaps part of the reason for this disparity is the perceived
512 inaccessibility of the technical language of PDE analysis. A major purpose of this work is to
513 make PDEs in general, and pattern formation in particular, more widely accessible, by showing
514 how to both parametrise and analyse PDEs using simple out-of-the-box techniques (conditional
515 logistic regression and eigenvector calculations respectively). Of course, the analysis using such
516 techniques is limited and much more can be done with PDEs than presented here (discussed
517 in Supplementary Appendix E), but we hope that it will present a starting point for those who
518 have hitherto avoided PDE formalisms.

519 An important assumption in our approach is that data are not highly temporally auto-
520 correlated (i.e. we assume in the Methods that the distribution of turning angles between
521 successive steps is approximately uniform). If one does have highly auto-correlated data, there
522 are various possible approaches. The simplest is by subsampling to remove autocorrelation.
523 In particular, if data are very high frequency (e.g. $\geq 1\text{Hz}$), then one can subsample at the
524 points where the animal turns (Potts *et al.*, 2018). However, if subsampling leads to data so
525 coarse that there are large changes in resource gradient between successive location fixes then
526 the approach used here is not appropriate for the data, owing to the “small τ ” requirement
527 (i.e. that the gradient of resources does not vary a lot over the distance an animal covers in

528 time τ ; see Section 2.1). One way around this may be to smooth the resource landscape so
529 that these large changes in resource gradient vanish. However, this is only appropriate if the
530 animals are likely to be responding to such spatially-averaged resources, which will depend on
531 the study population.

532 Another way to deal with non-uniform turning angle distributions is to use the approach
533 of Patlak (1953), popularised by Turchin (1998), to arrive at a diffusion-taxis equation that
534 corrects for the autocorrelation. However, this itself is only an approximate correction, and can
535 be inaccurate when combined with biased movement (Wang & Potts, 2017). A more accurate
536 PDE approximation to a correlated random walk is the telegrapher's equation (Masoliver *et al.*,
537 1993), which generalises the advection-diffusion formalism. However, this still does not give
538 an exact description of correlated movement in two dimensions. The extent to which either
539 the telegrapher's or the Patlak-Turchin approximations accurately capture the probability dis-
540 tribution of autocorrelated animal movement through heterogeneous environments is, to our
541 knowledge, an open question, and requires significant investigation beyond the scope of the
542 present study.

543 Away from step selection, the formalism of stochastic differential equations (SDEs) has been
544 used to deal with autocorrelated data, by modelling the velocity of the animal as a stochastic
545 process (Johnson *et al.*, 2008a). Here, exact inference is possible (Parton *et al.*, 2016), and
546 applications have been made to heterogeneous environments (Russell *et al.*, 2018). Further-
547 more, such SDEs often have probability density functions (PDFs) that evolve according to an
548 advection-diffusion PDE (Risken, 1996). However, since these SDEs describe the velocity of
549 an object, the resulting PDEs describe the PDF of the velocities, not the locations. To de-
550 scribe the locational PDF, i.e. space-use distribution, from a velocity-based stochastic process
551 is technically demanding and typically requires approximate techniques (Codling & Hill, 2005).

552 Animal movement through heterogeneous landscapes has also been studied using locational
553 SDEs, with a potential function modelling the taxis in response to the environment (Preisler
554 *et al.*, 2013). This has a direct connection to our PDE formalism (Equation 3). Specifically,

555 by setting the potential function in Preisler *et al.* (2013, Equation 2) to $-\beta \cdot \mathbf{Z}$ and employing
556 independent Brownian motions in each spatial direction, the resulting SDE has a PDF that is
557 described by Equation (3) (Risken, 1996). Like our SSA-PDE approach, the SDE of Preisler
558 *et al.* (2013) also has a convenient and efficient fitting procedure via regression techniques.
559 In this way, the diffusion-taxis PDEs described here offer a formal link between step selection
560 approaches and SDE approaches, which have hitherto had rather separate histories of technical
561 development.

562 It is also possible to incorporate autocorrelation in the approach of Preisler *et al.* (2013)
563 by choosing a correlated stochastic process for the noise term ($d\mathbf{V}(t)$ in Preisler *et al.* (2013)).
564 However, by doing this, the PDF is no longer exactly described by an advection-diffusion
565 equation (Risken, 1996).

566 Our use of SSA to parametrise PDEs relies on a limiting approximation that can affect
567 inference. From Fig. 1c, we see that SSA tends to perform well for relatively small time-step,
568 τ , but will overestimate the parameters in the PDE model as τ is increased. This is because the
569 PDE moves according to the local resource gradient, merely examining the pixels adjacent to
570 the current location. However, SSA compares the empirical ‘next location’ with a selection of
571 control locations, which are highly likely to contain pixels that are not adjacent to the current
572 location. This means that the movement decision may appear to be more strongly selected for
573 than is really the case. This corroborates the idea that discretisation can lead to overestimation
574 of selection, observed in recent theoretical work (Schlägel & Lewis, 2016b,a).

575 These issues of scale arise because the PDE framework in our study assumes movement along
576 a resource gradient. One could also build a PDE model to account for attraction to resources at
577 a distance, which is often ecologically relevant. For example, a switching Ornstein-Uhlenbeck
578 model of resource-driven movement, such as that of Wang *et al.* (2019), has a probability
579 distribution that evolves according to an advection-diffusion equation. It would be interesting
580 future work to extend the framework here to incorporate such models.

581 Acknowledgements

582 JRP thanks the School of Mathematics and Statistics at the University of Sheffield for grant-
583 ing him study leave which has enabled the research presented here. UES was supported by
584 the German Research Foundation in the framework of the BioMove Research Training Group
585 (DFG-GRK 2118/1). We thank the associate editor, Luca Börger, and two anonymous review-
586 ers for comments that have helped improve this manuscript.

587 Authors' contributions

588 JRP conceived and designed the research. JRP performed the research, with help from UES
589 regarding modelling the bank vole study. JRP wrote the first draft of the manuscript, and
590 both authors contributed substantially to revisions.

591 Data availability

592 No unpublished data were used in this study. Some results from Schlägel *et al.* (2019) were
593 used, which can be obtained directly from Schlägel *et al.* (2019).

594 References

- 595 1.
596 Ames, W.F. (2014). *Numerical methods for partial differential equations*. Academic press,
597 San Diego.
- 598 2.
599 Avgar, T., Potts, J.R., Lewis, M.A. & Boyce, M.S. (2016). Integrated step selection analysis:
600 bridging the gap between resource selection and animal movement. *Methods Ecol. Evol.*, 7,
601 619–630.

- 602 3.
603 Barnett, A. & Moorcroft, P. (2008). Analytic steady-state space use patterns and rapid
604 computations in mechanistic home range analysis. *J. Math. Biol.*, 57, 139–159.
- 605 4.
606 Baurmann, M., Gross, T. & Feudel, U. (2007). Instabilities in spatially extended predator–
607 prey systems: Spatio-temporal patterns in the neighborhood of turing–hopf bifurcations. *J.*
608 *Theor. Biol.*, 245, 220–229.
- 609 5.
610 Cantrell, R.S. & Cosner, C. (2004). *Spatial ecology via reaction-diffusion equations*. John
611 Wiley & Sons, Chichester.
- 612 6.
613 Chesson, P.L. (1985). Coexistence of competitors in spatially and temporally varying envi-
614 ronments: a look at the combined effects of different sorts of variability. *Theor. Pop. Biol.*,
615 28, 263–287.
- 616 7.
617 Codling, E. & Hill, N. (2005). Calculating spatial statistics for velocity jump processes with
618 experimentally observed reorientation parameters. *J. Math. Biol.*, 51, 527–556.
- 619 8.
620 Durrett, R. & Levin, S. (1994). The importance of being discrete (and spatial). *Theor. Pop.*
621 *Biol.*, 46, 363–394.
- 622 9.
623 Eftimie, R., De Vries, G. & Lewis, M. (2007). Complex spatial group patterns result from
624 different animal communication mechanisms. *P. Natl. Acad. Sci. USA*, 104, 6974–6979.
- 625 10.

626 Eftimie, R., de Vries, G. & Lewis, M. (2009). Weakly nonlinear analysis of a hyperbolic
627 model for animal group formation. *J. Math. Biol.*, 59, 37–74.

628 11.

629 Evans, L.C. (2010). *Partial differential equations*. American Mathematical Society, Provi-
630 dence, Rhode Island.

631 12.

632 Fagan, W.F., Lewis, M.A., Auger-Méthé, M., Avgar, T., Benhamou, S., Breed, G., LaDage,
633 L., Schlägel, U.E., Tang, W.w., Papastamatiou, Y.P., Forester, J. & Mueller, T. (2013).
634 Spatial memory and animal movement. *Ecol. Lett.*, 16, 1316–1329.

635 13.

636 Ferguson, E.A. (2018). *Modelling collective movement across scales: from cells to wildebeest*.
637 Ph.D. thesis, University of Glasgow.

638 14.

639 Ferguson, E.A., Matthiopoulos, J., Insall, R.H. & Husmeier, D. (2016). Inference of the
640 drivers of collective movement in two cell types: Dictyostelium and melanoma. *J. Roy. Soc.*
641 *Interface*, 13, 20160695.

642 15.

643 Forester, J., Im, H. & Rathouz, P. (2009). Accounting for animal movement in estimation
644 of resource selection functions: sampling and data analysis. *Ecology*, 90, 3554–3565.

645 16.

646 Fortin, D., Beyer, H., Boyce, M., Smith, D., Duchesne, T. & Mao, J. (2005). Wolves influence
647 elk movements: Behavior shapes a trophic cascade in yellowstone national park. *Ecology*,
648 86, 1320–1330.

649 17.

650 Garlick, M.J., Powell, J.A., Hooten, M.B. & McFarlane, L.R. (2011). Homogenization of
651 large-scale movement models in ecology. *Bull. Math. Biol.*, 73, 2088–2108.

652 18.

653 Giuggioli, L., Sevilla, F.J. & Kenkre, V. (2009). A generalized master equation approach to
654 modelling anomalous transport in animal movement. *J. Phys. A: Math. Theor.*, 42, 434004.

655 19.

656 Gosling, L.M. & Roberts, S.C. (2001). Scent-marking by male mammals: cheat-proof signals
657 to competitors and mates. In: *Advances in the Study of Behavior*. Elsevier, vol. 30, pp.
658 169–217.

659 20.

660 Hays, G.C., Ferreira, L.C., Sequeira, A.M., Meekan, M.G., Duarte, C.M., Bailey, H., Bailleul,
661 F., Bowen, W.D., Caley, M.J., Costa, D.P. *et al.* (2016). Key questions in marine megafauna
662 movement ecology. *Trends Ecol. Evol.*, 31, 463–475.

663 21.

664 Hefley, T.J., Hooten, M.B., Russell, R.E., Walsh, D.P. & Powell, J.A. (2017). When mech-
665 anism matters: Bayesian forecasting using models of ecological diffusion. *Ecol. Lett.*, 20,
666 640–650.

667 22.

668 Holgate, P. (1971). Random walk models for animal behavior. In: *Statistical ecology: sam-
669 pling and modeling biological populations and population dynamics, vol. 2* (eds. Patil, G.,
670 Pielou, E. & Walters, W.). Penn State University Press, University Park, PA.

671 23.

672 Johnson, C. (2012). *Numerical solution of partial differential equations by the finite element
673 method*. Dover Publications, New York.

674 24.

675 Johnson, D.S., London, J.M., Lea, M.A. & Durban, J.W. (2008a). Continuous-time corre-
676 lated random walk model for animal telemetry data. *Ecology*, 89, 1208–1215.

677 25.

678 Johnson, D.S., Thomas, D.L., Ver Hoef, J.M. & Christ, A. (2008b). A general framework
679 for the analysis of animal resource selection from telemetry data. *Biometrics*, 64, 968–976.

680 26.

681 Klausmeier, C.A. (1999). Regular and irregular patterns in semiarid vegetation. *Science*,
682 284, 1826–1828.

683 27.

684 Kondo, S. & Miura, T. (2010). Reaction-diffusion model as a framework for understanding
685 biological pattern formation. *Science*, 329, 1616–1620.

686 28.

687 Kot, M., Lewis, M.A. & van den Driessche, P. (1996). Dispersal data and the spread of
688 invading organisms. *Ecology*, 77, 2027–2042.

689 29.

690 Levin, S.A. (1974). Dispersion and population interactions. *Am. Nat.*, 108, 207–228.

691 30.

692 Lewis, M. & Moorcroft, P. (2006). *Mechanistic Home Range Analysis*. Princeton University
693 Press, Princeton University Press, Princeton, USA.

694 31.

695 Lewis, M.A. & Murray, J.D. (1993). Modelling territoriality and wolf-deer interactions.
696 *Nature*, 366, 738–740.

697 32.

698 Lewis, M.A., Petrovskii, S.V. & Potts, J.R. (2016). *The mathematics behind biological inva-*
699 *sions*. Springer, Switzerland.

700 33.

701 Li, X., Jiang, W. & Shi, J. (2013). Hopf bifurcation and Turing instability in the reaction-
702 diffusion Holling-Tanner predator-prey model. *IMA J. Appl. Math.*, 78, 287–306.

703 34.

704 Macandza, V.A., Owen-Smith, N. & Cain III, J.W. (2012). Dynamic spatial partitioning
705 and coexistence among tall grass grazers in an African savanna. *Oikos*, 121, 891–898.

706 35.

707 Macdonald, B. & Husmeier, D. (2015). Computational inference in systems biology. In:
708 *International Conference on Bioinformatics and Biomedical Engineering*. Springer, pp. 276–
709 288.

710 36.

711 Masoliver, J., Porra, J.M. & Weiss, G.H. (1993). Some two and three-dimensional persistent
712 random walks. *Physica A*, 193, 469–482.

713 37.

714 Michelot, T., Blackwell, P.G. & Matthiopoulos, J. (2018). Linking resource selection and
715 step selection models for habitat preferences in animals. *Ecology*, 100, e02452.

716 38.

717 Moorcroft, P. & Barnett, A. (2008). Mechanistic home range models and resource selection
718 analysis: a reconciliation and unification. *Ecology*, 89, 1112–1119.

719 39.

720 Moorcroft, P.R., Lewis, M.A. & Crabtree, R.L. (2006). Mechanistic home range models
721 capture spatial patterns and dynamics of coyote territories in Yellowstone. *Proc. Roy. Soc.*
722 *B*, 273, 1651–1659.

- 723 40.
724 Morales, J.M., Moorcroft, P.R., Matthiopoulos, J., Frair, J.L., Kie, J.G., Powell, R.A.,
725 Merrill, E.H. & Haydon, D.T. (2010). Building the bridge between animal movement and
726 population dynamics. *Phil. Trans. R. Soc. Lond. B*, 365, 2289–2301.
- 727 41.
728 Murray, J.D. (1981). A pre-pattern formation mechanism for animal coat markings. *J.*
729 *Theor. Biol.*, 88, 161–199.
- 730 42.
731 Murray, J.D. (2003). *Mathematical biology II: Spatial models and biomedical applications.*
732 Springer-Verlag, New York.
- 733 43.
734 Murray, J.D. (2012). *Asymptotic analysis.* vol. 48. Springer Science & Business Media.
- 735 44.
736 Nakamasu, A., Takahashi, G., Kanbe, A. & Kondo, S. (2009). Interactions between zebrafish
737 pigment cells responsible for the generation of turing patterns. *P. Natl. Acad. Sci. USA*, 106,
738 8429–8434.
- 739 45.
740 Ovaskainen, O. (2004). Habitat-specific movement parameters estimated using mark–
741 recapture data and a diffusion model. *Ecology*, 85, 242–257.
- 742 46.
743 Ovaskainen, O., Rekola, H., Meyke, E. & Arjas, E. (2008). Bayesian methods for analyzing
744 movements in heterogeneous landscapes from mark–recapture data. *Ecology*, 89, 542–554.
- 745 47.
746 Painter, K.J. & Hillen, T. (2015). Navigating the flow: individual and continuum models for
747 homing in flowing environments. *J. Roy. Soc. Interface*, 12, 20150647.

748 48.

749 Parton, A., Blackwell, P.G. & Skarin, A. (2016). Bayesian inference for continuous time
750 animal movement based on steps and turns. In: *International Conference on Bayesian*
751 *Statistics in Action*. Springer, pp. 223–230.

752 49.

753 Patlak, C.S. (1953). Random walk with persistence and external bias. *The bulletin of*
754 *mathematical biophysics*, 15, 311–338.

755 50.

756 Petrovskii, S.V., Morozov, A.Y. & Venturino, E. (2002). Allee effect makes possible patchy
757 invasion in a predator–prey system. *Ecol. Lett.*, 5, 345–352.

758 51.

759 Potts, J., Bastille-Rousseau, G., Murray, D., Schaefer, J. & Lewis, M. (2014). Predicting
760 local and non-local effects of resources on animal space use using a mechanistic step-selection
761 model. *Methods Ecol. Evol.*, 5, 253–262.

762 52.

763 Potts, J.R., Börger, L., Scantlebury, D.M., Bennett, N.C., Alagaili, A. & Wilson, R.P. (2018).
764 Finding turning-points in ultra-high-resolution animal movement data. *Methods Ecol. Evol.*,
765 9, 2091–2101.

766 53.

767 Potts, J.R. & Lewis, M.A. (2014). How do animal territories form and change? lessons from
768 20 years of mechanistic modelling. *Proc. Roy. Soc. B*, 281, 20140231.

769 54.

770 Potts, J.R. & Lewis, M.A. (2016a). How memory of direct animal interactions can lead to
771 territorial pattern formation. *J. Roy. Soc. Interface*, 13, 20160059.

772 55.

773 Potts, J.R. & Lewis, M.A. (2016b). Territorial pattern formation in the absence of an
774 attractive potential. *J Math. Biol.*, 72, 25–46.

775 56.

776 Potts, J.R. & Lewis, M.A. (2019). Spatial memory and taxis-driven pattern formation in
777 model ecosystems. *Bull. Math. Biol.*, 81, 2725–2747.

778 57.

779 Powell, J.A. & Zimmermann, N.E. (2004). Multiscale analysis of active seed dispersal con-
780 tributes to resolving reid’s paradox. *Ecology*, 85, 490–506.

781 58.

782 Preisler, H.K., Ager, A.A. & Wisdom, M.J. (2013). Analyzing animal movement patterns
783 using potential functions. *Ecosphere*, 4, 1–13.

784 59.

785 Riotte-Lambert, L., Benhamou, S., Bonenfant, C. & Chamaillé-Jammes, S. (2017). Spa-
786 tial memory shapes density dependence in population dynamics. *Proc. Roy. Soc. B*, 284,
787 20171411.

788 60.

789 Risken, H. (1996). *The Fokker-Planck Equation*. Springer.

790 61.

791 Roques, L. (2013). *Modèles de réaction-diffusion pour l’écologie spatiale: Avec exercices*
792 *dirigés*. Editions Quae.

793 62.

794 Russell, J.C., Hanks, E.M., Haran, M., Hughes, D. *et al.* (2018). A spatially varying stochas-
795 tic differential equation model for animal movement. *Ann. Appl. Stat.*, 12, 1312–1331.

796 63.

797 Schlägel, U.E. & Lewis, M.A. (2016a). A framework for analyzing the robustness of movement
798 models to variable step discretization. *J. Math. Biol.*, 73, 815–845.

799 64.

800 Schlägel, U.E. & Lewis, M.A. (2016b). Robustness of movement models: can models bridge
801 the gap between temporal scales of data sets and behavioural processes? *J. Math. Biol.*, 73,
802 1691–1726.

803 65.

804 Schlägel, U.E., Signer, J., Herde, A., Eden, S., Jeltsch, F., Eccard, J.A. & Dammhahn,
805 M. (2019). Estimating interactions between individuals from concurrent animal movements.
806 *Methods Ecol. Evol.*

807 66.

808 Sherratt, J.A. (2005). An analysis of vegetation stripe formation in semi-arid landscapes. *J.*
809 *Math. Biol.*, 51, 183–197.

810 67.

811 Signer, J., Fieberg, J. & Avgar, T. (2017). Estimating utilization distributions from fitted
812 step-selection functions. *Ecosphere*, 8, e01771.

813 68.

814 Signer, J., Fieberg, J. & Avgar, T. (2019). Animal movement tools (amt): R package for
815 managing tracking data and conducting habitat selection analyses. *Ecol. Evol.*, 9, 880–890.

816 69.

817 Spiegel, O., Leu, S.T., Bull, C.M. & Sih, A. (2017). What's your move? movement as a link
818 between personality and spatial dynamics in animal populations. *Ecol. Lett.*, 20, 3–18.

819 70.

820 Thurfjell, H., Ciuti, S. & Boyce, M. (2014). Applications of step-selection functions in ecology
821 and conservation. *Mov. Ecol.*, 2, 4.

822 71.

823 Topaz, C.M., Bertozzi, A.L. & Lewis, M.A. (2006). A nonlocal continuum model for biological
824 aggregation. *Bull. Math. Biol.*, 68, 1601.

825 72.

826 Tulumello, E., Lombardo, M.C. & Sammartino, M. (2014). Cross-diffusion driven instability
827 in a predator-prey system with cross-diffusion. *Acta Appl. Math.*, 132, 621–633.

828 73.

829 Turchin, P. (1998). *Quantitative analysis of movement: measuring and modeling population*
830 *redistribution in animals and plants*. vol. 1. Sinauer Associates Sunderland, Massachusetts,
831 USA.

832 74.

833 Turing, A.M. (1952). The chemical basis of morphogenesis. *Phil. Trans. R. Soc. Lond. B*,
834 237, 37–72.

835 75.

836 Vanak, A., Fortin, D., Thakera, M., Ogdene, M., Owena, C., Greatwood, S. & Slotow, R.
837 (2013). Moving to stay in place - behavioral mechanisms for coexistence of african large
838 carnivores. *Ecology*, 94, 2619–2631.

839 76.

840 Wang, Y., Blackwell, P., Merkle, J. & Potts, J. (2019). Continuous time resource selection
841 analysis for moving animals. *Methods Ecol. Evol.*

842 77.

843 Wang, Y.S. & Potts, J.R. (2017). Partial differential equation techniques for analysing animal
844 movement: A comparison of different methods. *Journal of Theoretical Biology*, 416, 52–67.

845 78.

846 Wijeyakulasuriya, D.A., Hanks, E.M., Shaby, B.A. & Cross, P.C. (2019). Extreme value-
847 based methods for modeling elk yearly movements. *J Agr. Biol. Envir. Stat.*, 24, 73–91.

848 79.

849 Wilson, K., Hanks, E. & Johnson, D. (2018). Estimating animal utilization densities using
850 continuous-time markov chain models. *Methods Ecol. Evol.*, 9, 1232–1240.

851 80.

852 Xun, X., Cao, J., Mallick, B., Maity, A. & Carroll, R.J. (2013). Parameter estimation of
853 partial differential equation models. *J. Am. Stat. Assoc.*, 108, 1009–1020.

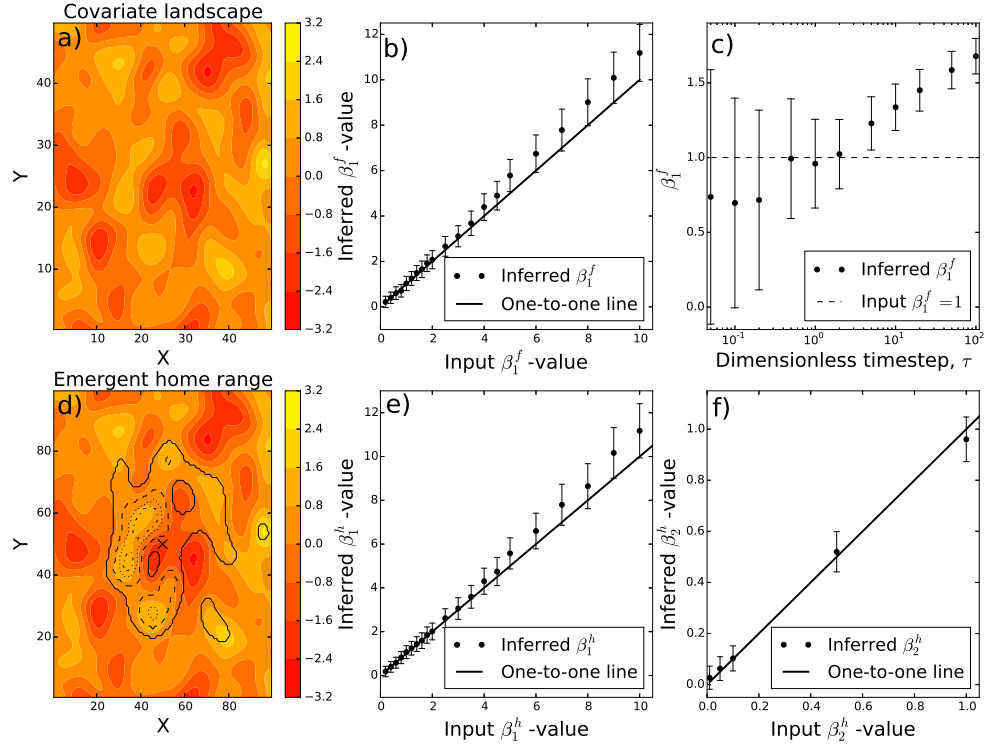


Fig. 1. Study on simulated data. Inference from simulated paths of individuals moving according to the diffusion-taxis Equation (5). Panel (a) shows a resource layer given by a Gaussian random field, with colour showing the value of the resource layer at each point. Panel (b) gives the result of using step selection analysis to parametrise the Fixed Resource model, where $Z_1^f(\mathbf{x})$ is given by this example layer. Dots give the inferred β_1^f -values, with bars giving 95% confidence intervals. Panel (c) shows how inference varies as the time-step between measured locations, τ is increased. Here, the value used to simulate the diffusion-taxis equation is $\beta_1^f = 1$. Panel (d) shows the emergent home range, as predicted by Equation (8), for the Home Range model with $\beta_1^h = 1$, $\beta_2^h = 0.1$. Here, β_1^h denotes the strength of the resource landscape's effect on movement and β_2^h denotes the tendency to move towards the attraction centre, \mathbf{x}_c (denoted by a cross). Details of this model are given in Section 2.2. The colour-filled contours are as in Panel (a) and the black curves show contours of the home range distribution. The solid black curve encloses 95% of the utilisation distribution. The 25%, 50%, and 75% kernels are given by dash-dot, dotted, and dashed curves respectively. Panels (e) and (f) show the results of using step selection analysis to infer β_1^h and β_2^h , in an identical format to Panels (b) and (c). Panel (e) has $\beta_2^h = 0.1$ fixed and Panel (f) has $\beta_1^h = 1$ fixed.

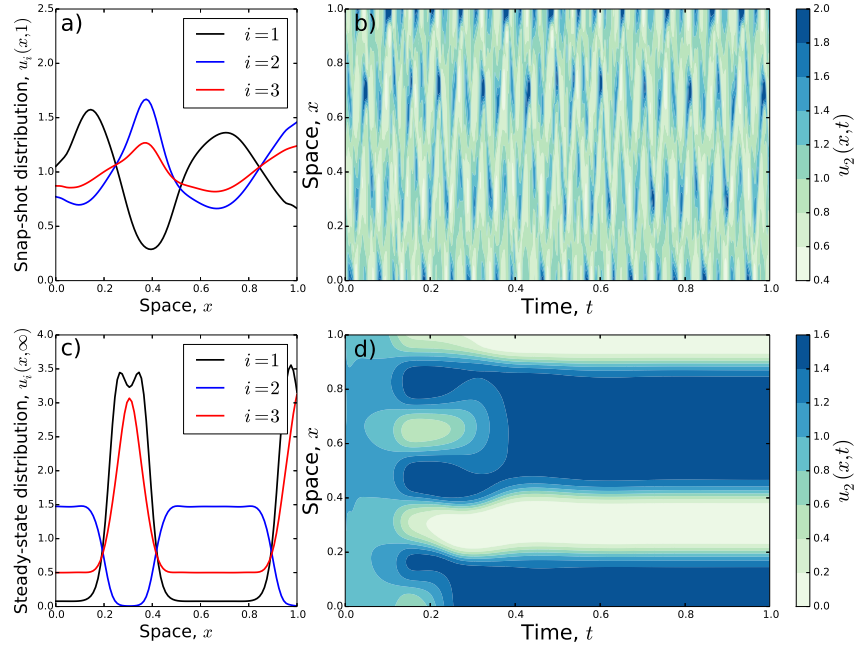


Fig. 2. Pattern formation from diffusion-taxis systems. Panels (a) and (b) give a numerical solution of the system in Equation (7) in a simple one dimensional example, with $M = 3$ individuals (indexed with the letter i), $\beta_{1,2}^v = -2$, $\beta_{1,3}^v = -0.5$, $\beta_{2,1}^v = 0.5$, $\beta_{2,3}^v = 2$, $\beta_{3,1}^v = 0.5$, $\beta_{3,2}^v = 0.5$. This is in the regime where linear pattern formation analysis predicts oscillatory patterns. Panel (a) gives a snap-shot of the system at $t = 1$, showing distributions of $u_1(x, 1)$, $u_2(x, 1)$, and $u_3(x, 1)$. Panel (b) shows the change in $u_2(x, t)$ over both space and time. We observe that the system never seems to settle to a steady state. This contrasts with Panels (c) and (d) which show a one dimensional example where linear pattern formation analysis predicts stationary patterns to emerge. Here, $M = 3$, $\beta_{1,2}^v = -2$, $\beta_{1,3}^v = -0.5$, $\beta_{2,1}^v = 0.5$, $\beta_{2,3}^v = -2$, $\beta_{3,1}^v = 0.5$, $\beta_{3,2}^v = 0.5$. Panel (c) gives the stationary distribution, whilst Panel (d) displays convergence of the system towards this stationary distribution, for $u_2(x, t)$. Throughout all panels, the spatial averaging kernel is $B(x) = (x - 0.05, x + 0.05)$ (see comment before Eqn. 7).

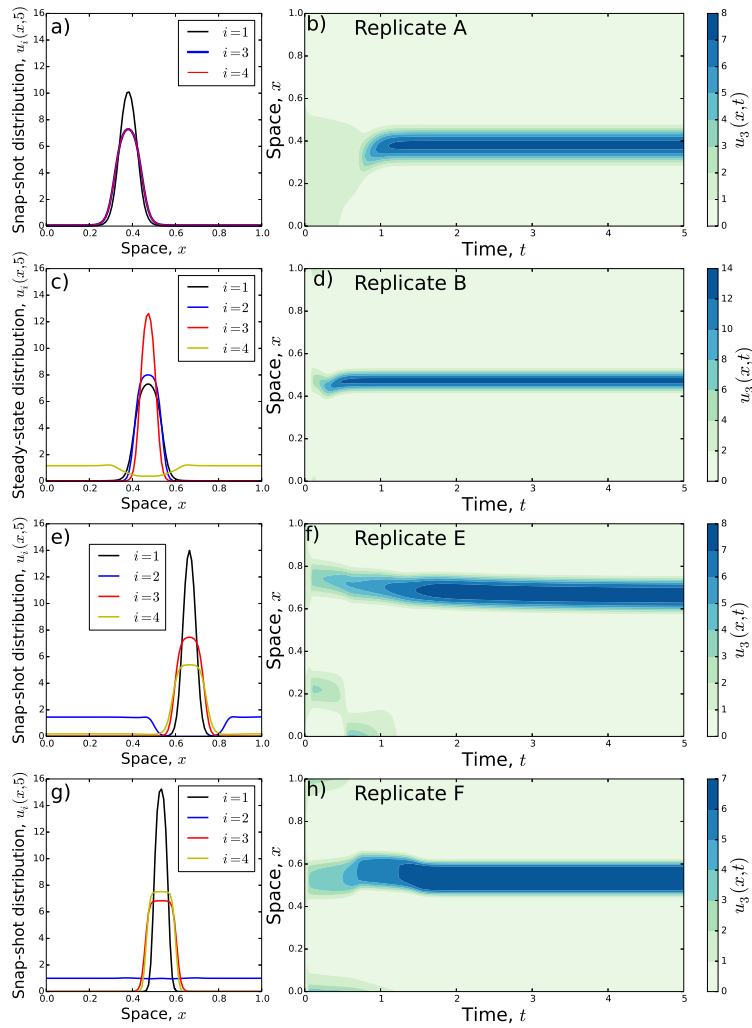


Fig. 3. Predictions of pattern formation properties of vole replicates. These plots demonstrate whether the patterns predicted by linear analysis correspond to aggregation and/or segregation between the constituent individuals (indexed with the letter i). Panels (a-b) correspond to Replicate A from Schlägel *et al.* (2019), (c-d) correspond to Replicate B, (e-f) to Replicate E, and (g-h) to Replicate F. Left-hand panels give the steady-state of the distribution after solving each diffusion-taxis system numerically, with initial conditions being a small random perturbation of the homogeneous steady state ($u_i(x) = 1$ for all i, x). These display the aggregation/segregation properties of the system. The right-hand panels give Individual 3's simulated probability distribution as it changes over time.